

Interaction of soft-x-ray thermal radiation with foam-layered targets

D. Batani,¹ T. Desai,¹ Th. Löwer,² T. A. Hall,³ W. Nazarov,⁴ M. Koenig,⁵
and A. Benuzzi-Mounaix⁵

¹*Dipartimento di Fisica “G. Occhialini” and INFN, Università di Milano-Bicocca, Piazza della Scienza 3, 20126 Milano, Italy*

²*Max Planck Institut für Quantenoptik, D-85740 Garching, Germany*

³*University of Essex, Wivenhoe Park, Colchester, Essex, CO4 3SQ, United Kingdom*

⁴*Department of Chemistry, University of Dundee, Scotland, United Kingdom*

⁵*LULI, UMR 7605 CEA-X-Paris VI, Ecole Polytechnique, 91128 Palaiseau, France*

(Received 10 September 2001; revised manuscript received 17 January 2002; published 13 June 2002)

We have studied the interaction of soft-x-ray thermal radiation with foam-layered metal targets. X-ray radiation was produced by focusing a high-energy laser inside a small size hohlraum. An increment in shock pressure, up to a factor of ≈ 4 for 50 mg/cm³ foam density, was observed with the foam layer as compared to bare metal targets. This follows from the propagation of radiation-driven shock wave in the foam and the impedance mismatch at the foam-payload interface.

DOI: 10.1103/PhysRevE.65.066404

PACS number(s): 52.50.Jm, 52.38.-r, 52.25.Os

INTRODUCTION

Recently, low-density porous materials, or “foams,” have found many applications in laser-plasma experiments, in particular related to inertial confinement fusion. In the direct drive approach, their use has been suggested to get an efficient thermal smoothing of laser energy deposition [1,2]: the so-called “foam-buffered targets” should help in relaxing the constraints on uniform laser irradiation, especially at early times (the well-known “imprint” problem).

One major problem in indirect drive is the hohlraum closure due to the inward motion of the high-Z plasma from the hohlraum wall [3]. A gas placed inside the hohlraum may constrain such motion, as proposed in Ref. [3] and studied, for instance, in Ref. [4]. In this context, a low-density foam can be an interesting alternative to the use of a gas: hence it is important to study the interaction of soft-x-ray thermal radiation with foams, in order to establish, in particular, the different interaction regimes. At very low foam densities, a supersonic ionization wave will propagate in the foam while, at higher densities, the formation of a shock is expected, with a velocity that, by definition, is only slightly supersonic. Since this will change the dynamics of the interaction and the time scales, it is very important to precisely define the transition between two such regimes.

Also it has been suggested that the total drive pressure can be increased by attaching a low-density foam onto the solid shell of the fusion capsule [5]. Willi *et al.* suggested that pressure increases because “the total pressure acting on the foil target is then the ablation pressure plus the material pressure of the heated foam plasma,” and studied the dynamics of foil-foam packages [6]. As diagnostics, they used time resolved shadowgraphy and followed the trajectory of the target. Targets with a foam layer were observed to start their motion with a certain delay but to get a stronger acceleration. Target motion was then simulated with the hydro code MEDUSA, and the pressure obtained from the code when the simulation matched experimental data.

The purpose of the experiment presented in this paper was to study the effect of low-density foams on the generation of

drive pressures: planar foil targets, with an overlayer of foam, were driven by soft x rays generated inside a gold hohlraum. Results were compared with those from bare metal targets to check the efficacy of the foam layer in indirect drive. Our experiment reproduced and complemented the study by Willi *et al.* However, we used a diagnostics that, in our opinion, is more direct and appropriate for the evaluation of shock pressures.

The method consists in measuring the shock velocity using a target with a step on rear side. The arrival of the shock at the base and at the step of the target heats the material and induces light emission. This can be space and time resolved with a streak camera allowing the shock velocity, D , in the step to be directly measured. The knowledge of the equation of state (EOS) of the material, and the use of Hugoniot-Rankine relations [7], allows the shock pressure to be obtained from the shock velocity. This method is easy and direct and it is largely used in laser-driven shock and EOS experiments [8]. Of course, if the shock is stationary it directly gives the “instantaneous” values of shock velocity and pressure. Otherwise, it gives average values over the time needed to the shock to cross the step (between 100 and 200 ps in our experimental conditions). This is probably what is happening here, since hydrodynamics simulations show a nonstationary shock with a complicated dynamics.

Also, our diagnostic is less sensitive to two-dimensional effects that affect target displacement at large times and, finally, assures a good precision in the measurement of the delay of shock arrival at the target rear side (i.e., the time when the target begins to move). As discussed later, the method allows the value of pressure to be determined with a typical error of $\approx 15\%$ in our experimental conditions. This is a small incertitude as compared to the large measured values of pressure amplification (of the order of ≤ 4).

EXPERIMENTAL SETUP

The experiment was performed using the Asterix laser at MPQ, Garching, which delivers a single beam (of diameter 30 cm) energy up to 400 J per pulse at a wavelength λ

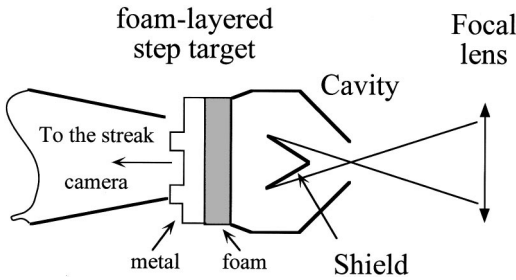


FIG. 1. Experimental setup showing the labyrinth cavity and the schematic representation of the target design.

$=0.44 \mu\text{m}$ (3ω of iodine laser) in a time $\tau_L \approx 450$ ps (full width at half maximum duration).

The laser was focused inside a small size hohlraum (cavity) to generate soft-x-ray Planckian radiation. Our hohlraum (called labyrinth cavity [9]) was designed to achieve high radiation temperatures, but also to optimize the irradiation uniformity with only one laser beam, and to minimize pre-heating of the target produced by direct primary x-rays. A shield with a conical shape has been constructed so that the laser irradiated area and the shocked material are not in direct view of each other (Fig. 1). The total inner surface of the hohlraum is equivalent to a sphere of 1 mm diameter (equivalent cavity radius $R_c = 0.5$ mm). The hohlraum has been made by electroplating and etching suitable brass mandrels and it is built from two parts fastened together.

Targets were fabricated with the following specifications. (1) aluminum base of thickness $h = 16.95 \mu\text{m}$ with an aluminum step of $6.23 \mu\text{m}$; or (2) gold base of thickness $h = 4.96 \mu\text{m}$ with a $1.95 \mu\text{m}$ gold step. The front gold surface was layered with low-density foam ($50 \mu\text{m}$ thick foam of density 20 mg/cm^3 , and 50 , 100 , and $150 \mu\text{m}$ thick foam of density 50 mg/cm^3). The corresponding areal densities were $\rho d = 0.1$, 0.25 , 0.5 , and 0.75 mg/cm^2 . Here ρ is the foam density and d is its thickness. Foams were realized at Dundee University [10]. The monomer used was TMPTA (trimethylol propane triacrylate, $\text{C}_{15}\text{H}_{20}\text{O}_6$). Starting from a monomer solution containing a photoinitiator, foams were polymerized *in situ* using UV light inside a brass ring of the required thickness, which determined the final foam thickness. The schematic representation of the targets is shown in Fig. 1.

A visible streak camera was used to record the shock breakout signal. The temporal resolution was better than 8 ps (as determined by the streak camera sweep speed and slit size). The system imaging the target rear face onto the streak slit had magnification $M = 10$, allowing a spatial resolution of better than $10 \mu\text{m}$. A protection tube [9] was used for the diagnostics light path, to shield the streak camera slit from scattered laser light.

EXPERIMENTAL RESULTS

The shock transit time provides the measure of the shock velocity D through the target rear step. For Al targets, the shock pressure was then evaluated by using the Sesame tables [11] and, for gold targets, the empirical scaling law proposed by Al'tshuler [12]. Indeed recent EOS measure-

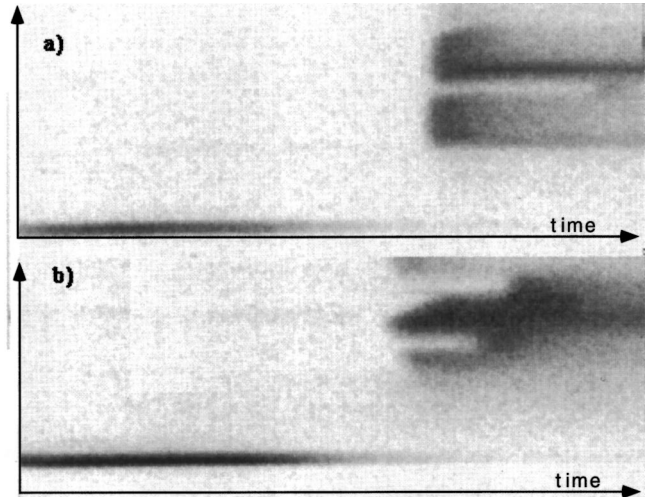


FIG. 2. Streak camera images of (a) Al target (b) foam-Au target. The dimensions of the image are 1 ns (horizontal) and $300 \mu\text{m}$ (vertical).

ments for gold [13] suggest that Sesame is not correct at high pressure. However, the use of Sesame tables would only slightly change the numerical value of pressure (the difference is within 10%) but not affect in any way our conclusions.

Figure 2(a) shows the streak camera image obtained with an Al target (shot no. 13027). In this case, the shock velocity measured in the aluminum step was 24.1 km/s , which corresponds to a shock pressure of about 9.6 Mbar. The signal on the left in Fig. 2 is a time fiducial: a part of the incoming laser beam is sent with an optical fiber onto the streak camera slit and synchronized so to give the arrival time of the laser pulse on target front side. The time interval Δt from the arrival of laser pulse maximum to the shock breakout on target rear side can then be measured from the streak image. Figure 2(b) shows the shock breakout from foam/gold target (shot no. 13026, foam of 50 mg/cm^3 and thickness $\approx 50 \mu\text{m}$). In this case the shock velocity is 14.1 km/s , corresponding to a pressure of 20.2 Mbar.

Figure 3 shows the pressures deduced from the shock velocity for Al and Au/foam targets. It can be seen that, in our experimental conditions, by increasing the foam density and thickness, shock pressures are enhanced. Figure 3 also shows the time delay Δt that is also bigger for larger density and thickness. (The time delay plotted here is the one relative to the foam thickness only, i.e., we have subtracted the shock transit time in the metal base, h/D .)

The error bars on shock pressure have been obtained by considering the precision in the determination of shock velocity D due to the streak camera temporal resolution, and the knowledge of the step thicknesses and roughness [8,13]. For the streak camera sweep speed we used the calibration made in Ref. [14]. Using a simple error propagation evaluation, and including reading errors, we determined a maximum error of $\pm 7\%$ on D , which implies an error of about $\pm 15\%$ on shock pressure. In some cases [see Fig. 2(b) for instance] the shocks obtained with foam layered targets were much less uniform for reasons that are yet to be understood.

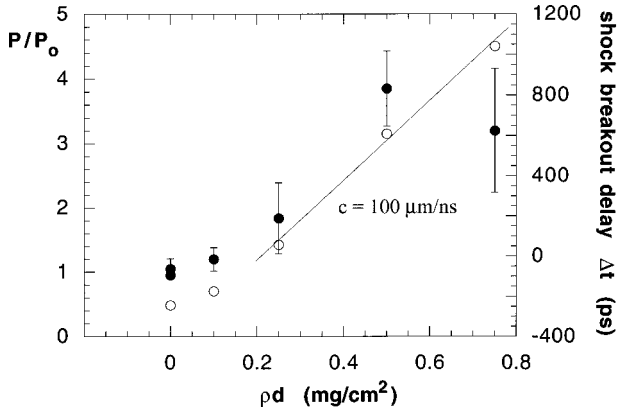


FIG. 3. Pressure increment, on the left (black circles), and delay of shock breakout (ps), on the right (white circles), vs foam layer areal density (mg/cm²). $\rho d=0$ corresponds to bare Al targets; $\rho d=0.1$ mg/cm² corresponds to a 20 mg/cm³, 50 μ m thick foam on Au; the other values to a 50 mg/cm³ foam on Au with thicknesses of 50, 100, and 150 μ m, respectively.

This reflects in larger error bars on shock velocity and shock pressure, which could be as large as $\pm 30\%$. Since the pressure amplification (≤ 4) is much larger than the experimental error bars ($\leq 30\%$), this does not affect our conclusion, indicating that foams are advantageous in order to obtain a pressure increase.

Concerning the delay of shock breakout, the error bars were much smaller since the elapsed times are much longer than the time required to the shock to cross the step. Again, we recall that pressure is obtained from the measurement of the step crossing time from which we calculate the velocity D and finally the pressure P . In the case of gold steps, this is obtained from the empirical scaling given by the empirical scaling law proposed by Al'tshuler *et al.* [12], according to which the relation between shock velocity D and fluid velocity U is: $D=3.15+1.47U$ (both measured in km/s). Pressure is then obtained by coupling this law to the equation $P=\rho_0UD$, which represents momentum conservation across the shock front (and is one of the Hugoniot-Rankine relations). Here ρ_0 is the density of gold (19.3 g/cm³).

DISCUSSION

In indirect drive, the radiation temperature is given by the well-known Boltzmann's law for blackbody radiation

$$T=(\eta E_L/4\pi R_c^2\tau_L\sigma)^{1/4}, \quad (1)$$

where σ is $=10^5$ when T is in eV, E_L the laser energy in I, R_c the cavity size in cm, and τ_L the pulse duration in seconds. In our case we get $T\approx 120$ eV at $E_L\approx 400$ J, in good agreement with direct experimental measurements [15]. The conversion efficiency into x rays was assumed $\eta\approx 80\%$, as appropriate for gold. When such radiation impinges on targets (without foam) it produces a pressure [9,14,16]

$$P(\text{Mbar})=44(\eta E_L/4\pi R_c^2\tau_x)^{10/13}t^{-3/26}, \quad (2)$$

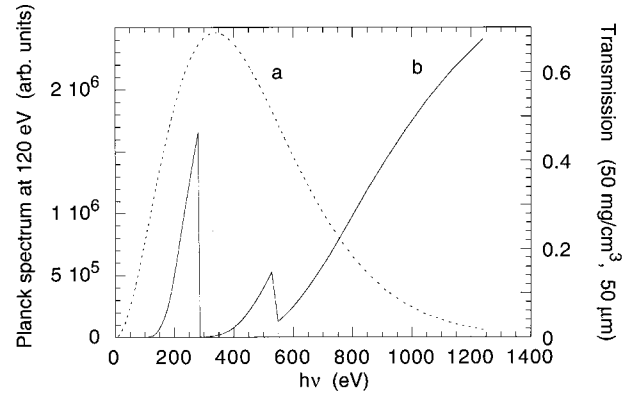


FIG. 4. Planckian spectrum corresponding to a temperature $T=120$ eV (a), and transparency of a 50 μ m, 50 mg/cm³ cold TMPTA foam (b).

where t is in ns and the quantity in brackets is in units of 10^{14} W/cm². Here τ_x is the duration of the x-ray pulse which is close to that of the laser pulse τ_L . There is no explicit dependence of the pressure on the target material, which implies that it is correct to compare the pressure obtained with Al and Au/foam targets, as done in Fig. 3. Hence not only the pressure increases with the thickness and the density of the foam, but also it is always larger than with bare targets. Equation (2) gives $P\approx 11$ Mbar for our typical experimental parameters, in fair enough agreement with our results on bare Al targets ($P\approx 9.6$ Mbar at $E_L\approx 290$ J).

What is the origin of the pressure increase with foam? Let us first notice that the foams are clearly undercritical to the thermal x-ray radiation. However, the foam is initially made of cold atoms that strongly absorb x rays by bound-bound transitions. Figure 4 shows a Planckian spectrum at 120 eV and the transparency of cold TMPTA foam [17]. Part of x rays are absorbed in the foam, ionizing it. As ionization goes on, the absorption coefficient reduces (for completely ionized foams it is only due to bremsstrahlung and recombination and is much smaller). The total energy spent in the ionization of the foam is of the order of

$$\Delta E=In_e\pi\Phi^2d/4, \quad (3)$$

where Φ is the diameter of the hohlraum hole to which the target is attached (400 μ m in our case) and I is the average ionization energy, which can be evaluated with an average atom model [18]. The average electron density in the foam is $n_e=\rho N_A Z/A$, assuming a complete ionization of the low- Z elements of the foam (as is likely to happen). Here N_A is Avogadro number, and Z and A are the average atomic number and weight of the foam ($Z\approx 3.85$, $A\approx 7.22$). In the case of 50 mg/cm³ we get $n_e=1.6\times 10^{22}$ cm⁻³. For $I\approx 10$ eV and $d=100$ μ m, we finally get $\Delta E\approx 0.3$ J, which must be compared with the fraction of the total x-ray energy (ηE_L) impinging on the hohlraum hole [$\eta E_L(\pi\Phi^2d/4)/(4\pi R_c^2)=12.8$ J] and shows that the ionization losses are negligible.

Two scenarios are then possible depending on foam density. If this is very low, an ionization wave propagates supersonically in the foam [19,20]. At the same time, a part of x-ray radiation penetrates practically free through the foam

to be abruptly absorbed at the Au-foam interface due to the much higher absorption of gold (higher Z and higher density). These are the harder x-rays ($h\nu > 1$ keV) but also those with energies just below the O and C absorption edges (see Fig. 4) (A similar behavior of x rays was observed in Ref. [2].) These produce ablation of gold and the generation of a shock. However, now the ablating gold plasma is confined due to the presence of foam, the plasma energy that would have been spent in motion of the plasma is retained as thermal energy of the confined plasma. Thus the total pressure is due to ablation of gold surface by (harder) x rays but also to gold plasma confinement (because of the presence of foam).

The situation is analogous to experiments where laser-driven shocks are confined by a layer of transparent material, as studied by Fabbro *et al.* [21]. The pressure increment should be given by the material pressure of the foam plasma

$$P_{\text{th}} = (Z + 1)n_i kT, \quad (4)$$

where k is Boltzmann's constant, and the average ion density is $n_i = \rho N_A / A$. In the case of 20 mg/cm^3 and $T = 120 \text{ eV}$ we find $P_{\text{th}} = 1.4 \text{ Mbar}$, against an experimental pressure increment $\approx 1.3 \text{ Mbar}$, or $P/P_0 \approx 1.1$, where P_0 is the average pressure experimentally obtained with bare metal targets (we must notice, however, that, due to the error bars, this difference, as well as the pressure amplification obtained in this case, is not really significant).

At higher foam densities, the scenario is quite different. Here a real radiation-driven shock is formed and propagates in the foam, reaches the interface with gold and undergoes a strong amplification due to impedance mismatch, i.e., the density difference between gold and foam (since the shock encounters a denser medium, a shock wave is reflected back into the foam, while the transmitted shock pressure is amplified [7]). This has been previously studied in direct drive [22,23]. Here the situation will be less "clean" because a radiative precursor is associated with the shock (due to the low density of the foam) and because some x rays will anyway reach the interface long before the shock arrival and produce some ablation and a local shock. Although weaker, this will interfere with the main radiation-driven shock inducing transient effects. However, shock impedance mismatch remains the driving factor.

The shock will need some time to reach its maximum velocity and a phase of steady state propagation. Hence, depending on the foam density and thickness, it may reach the interface before or after it has got its maximum pressure. Again, this was shown in direct-drive experiments. The shock pressure amplification will be given by [22]

$$\begin{aligned} P/P_0 &= 4\rho_{\text{Au}}/(\rho^{1/2} + \rho_{\text{Au}}^{1/2})^2, & t > \tau, \\ P/P_0 &= (P/P_0)_{\text{stat}}(8\rho/P_0)^{1/2}d\tau, & t < \tau, \end{aligned} \quad (5)$$

where $(P/P_0)_{\text{stat}}$ is the stationary value of P/P_0 , i.e., the one which is reached for $t > \tau$ as given by the first of the two equations, and where τ is the shock build-up time that is of the order of the laser pulse duration (see Ref. [22] for a detailed discussion). The maximum shock amplification that

can be obtained with a 50 mg/cm^3 foam is then $P/P_0 \approx 3.6$, and approaches 4 as the foam density ρ goes to 0.

In our experimental conditions, the transition between the two scenarios may probably take place between 20 and 50 mg/cm^3 . Indeed the fraction of the x-ray energy directly transmitted to the foam/metal interface varies from 36%, for 20 mg/cm^3 and $50 \mu\text{m}$, to about 1% for 50 mg/cm^3 and $150 \mu\text{m}$. Although only qualitative, being calculated using the absorption coefficients of the cold foam, these values seem to suggest a change of regime.

At the same time, the pressure increment in the case of 50 mg/cm^3 foam is much bigger than the material pressure while, within our error bars, it is in fair agreement with the maximum amplification expected from impedance mismatch ($P/P_0 \leq 4$). But the decisive point is the experimental observation of the shock delay Δt . From Fig. 3, the delay in the shock breakout scales linearly with foam thickness, for the case of 50 mg/cm^3 density, and the slope of the linear interpolation gives a velocity of $\approx 100 \mu\text{m/ns}$. This corresponds to the order expected for a shock wave and does not match with the hypothesis of a supersonic ionization wave. (Also, in the foam-confinement scenario, a shock is generated at the interface by x rays penetrating practically instantaneously, so that a large shock breakout delay seems difficult to be justified.) This conclusion seems to be in disagreement with Willi *et al.* who refer to the first scenario even in the case of a 100 mg/cm^3 foam (let us notice that, despite the smaller laser energy, due to the small size of our hohlraum, the temperature is practically the same as in their work).

Also the case of 50 mg/cm^3 and $50 \mu\text{m}$ corresponds to a nonstationary shock, as can be seen by looking at the delay in shock breakout ($\Delta t < 0$ implies that the shock reaches the interface before the full laser pulse energy has been deposited on target). In this case, by applying Eq. (5), we approximately recover the experimental value of the pressure amplification P/P_0 (≈ 2.2).

Finally, we must recall that the hot foam plasma will quickly expand, thereby reducing the pressure increase. Hence the foam should be sufficiently thick because, for very thin foam, the rarefaction wave will arrive at the rear surface of the foil very rapidly. This dictates a lower limit on the foil thickness, in order to maintain the pressure increase.

Just to give an order of magnitude, we can calculate that the sound velocity for a fully ionized plasma at 120 eV is $c_s \approx 10^7 \text{ cm/s}$. The rarefaction time can be estimated as $t \approx d/c_s \approx 500 \text{ ps}$ for a $50 \mu\text{m}$ thick foam. This must be compared with the shock transit time in the metal target, which is $\approx 6.91 \mu\text{m}/D \approx 638 \text{ ps}$ for $\rho d = 0.1 \text{ mg/cm}^2$ (using the measured values of the shock velocity D). The fact that the rarefaction and shock transit times are comparable, means that the foam plasma has the time to expand to approximately the double its original thickness during the shock transit in the metal target, thereby effectively reducing its average density. This may explain why the pressure increase observed with $\rho = 20 \text{ mg/cm}^3$, $d = 50 \mu\text{m}$ is slightly smaller than what calculated from material pressure (however, as said before, due to the large error bars, the difference and the value of pressure amplification itself are not significant in this case). For thicker targets, rarefaction is not important in our experimental conditions.

CONCLUSIONS

We have shown how shock pressure can be amplified in x-ray driven foam-layered targets. At very low foam densities, a supersonic ionization wave is produced and the pressure amplification is due to the foam plasma applying a material pressure on the ablating target plasma and effectively confining it. For denser foams, a real shock propagates in the foam and the pressure increase is due to impedance mismatch at the foam-metal interface, as previously observed in directly driven foam-metal targets [23]. At $\rho = 50 \text{ mg/cm}^3$, our measurements imply that the mechanism at work is the

second one, giving a pressure amplification as large as ≤ 4 . In both cases, amplification is dependent on the foam density and on the foam thickness.

ACKNOWLEDGMENTS

This experiment was performed at MPQ and fully supported by the EU in the framework of the Program "Access to Large Scale Facilities." We warmly acknowledge the help of the Asterix laser technical team. One of the authors (T.D.) acknowledges the support of the TRIL program of the ICTP, Trieste, and of INFM, Italy.

-
- [1] M. Dunne *et al.*, Phys. Rev. Lett. **75**, 3858 (1995); M. Desselberger *et al.*, *ibid.* **74**, 2961 (1995); D. Hoarty *et al.*, *ibid.* **78**, 3322 (1997); D. Batani *et al.*, Plasma Phys. Controlled Fusion **40**, 1567 (1998).
- [2] D. Batani *et al.*, Phys. Rev. E **62**, 8573 (2000).
- [3] J. Lindl, Phys. Plasmas **2**, 3933 (1995).
- [4] S. Glenzer *et al.*, Phys. Rev. Lett. **80**, 2845 (1998).
- [5] O. Willi *et al.*, Nucl. Fusion **40**, 537 (2000).
- [6] O. Willi *et al.*, in *Proceedings of the First International Conference on Inertial Fusion Science and Applications, Bordeaux*, edited by C. Labaune *et al.* (Elsevier, Paris, 1999), p. 122.
- [7] Ya. B. Zeldovich and Yu. P. Raizer, *Physics of Shock Waves and High Temperature Hydrodynamic Phenomena* (Academic, New York, 1967); S. Eliezer, A. Ghatak, and H. Hora, *An Introduction to Equations of State: Theory and Applications* (Cambridge University Press, Cambridge, England, 1986).
- [8] D. Batani *et al.*, Europhys. News **27**, 210 (1996); M. Koenig *et al.*, Phys. Rev. Lett. **74**, 2260 (1995).
- [9] A. Benuzzi *et al.*, Phys. Rev. E **54**, 2162 (1996).
- [10] J. Falconer *et al.*, J. Vac. Sci. Technol. A **13**, 1941 (1995).
- [11] SESAME Report on the Los Alamos Equation-of-State Library, Report No. LALP-83-4 (T4 Group LANL, Los Alamos, 1983).
- [12] L. V. Al'tshuler *et al.*, Zh. Prikl. Mekh. Tekhn. Fiz, **2**, 3 (1981) [J. Appl. Mech. Tech. Phys. **22**, 145 (1981)]; Sov. Phys. JETP **34**, 614 (1958).
- [13] D. Batani *et al.*, Phys. Rev. B **61**, 9287 (2000).
- [14] Th. Lower *et al.*, Phys. Rev. Lett. **72**, 3186 (1994).
- [15] I. B. Foldes *et al.*, Phys. Rev. E **64**, 016410 (2001).
- [16] R. Sigel, in *Laser Plasma Interactions 4*, Proceedings of the Thirty-fifth Scottish Universities Summer School in Physics, edited by M. B. Hooper (SUSSP, Edinburgh, 1988).
- [17] Marcus Wollbrecht, RATP, mvollbr@froentgen.physikk.uni-jena.de; B. Henke, in *X-Ray Data Booklet* (Lawrence Berkeley Laboratory, University of California, Berkeley, 1986).
- [18] Y. T. Lee and R. M. More, Phys. Fluids **27**, 1273 (1984).
- [19] J. Massen *et al.*, Phys. Rev. E **50**, 5130 (1994).
- [20] D. Hoarty *et al.*, Phys. Plasmas **6**, 2171 (1999); D. Hoarty *et al.*, Phys. Rev. Lett. **82**, 3070 (1999).
- [21] R. Fabbro *et al.*, J. Appl. Phys. **68**, 775 (1990).
- [22] D. Batani *et al.*, Phys. Rev. E **63**, 46 410 (2001); M. Temporal *et al.*, Eur. Phys. J. D **12**, 509 (2000).
- [23] A. Benuzzi *et al.*, Phys. Plasmas **5**, 2827 (1998).